



Contents lists available at ScienceDirect



Catalysis Today

journal homepage: www.elsevier.com/locate/cattod

Mesostructured vanadia–alumina catalysts for the synthesis of vitamin K₃

M. Florea*, R.S. Marin, F.M. Pălașanu, F. Neațu, V.I. Pârvulescu

University of Bucharest, Faculty of Chemistry, Department of Organic Chemistry, Biochemistry and Catalysis, 4–12 Regina Elisabeta Blvd., Bucharest 030016, Romania

ARTICLE INFO

Article history:

Received 7 September 2014

Received in revised form

15 December 2014

Accepted 19 December 2014

Available online xxx

Keywords:

Selective oxidation of 2-methylnaphthalene

Mesoporous vanadia–alumina oxides

Synthesis of vitamin K₃

ABSTRACT

Liquid-phase selective oxidation of 2-methylnaphthalene to the vitamin K₃ was investigated on a series of mesostructured vanadia–alumina catalysts with different V/Al ratios (0.1–1). They were prepared by the co-precipitation of ammonium metavanadate and aluminum nitrate at pH 5 and characterized by XRD, Raman, TG-DTA, elemental analysis and adsorption-desorption isotherms of nitrogen at –196 °C. The influence of the catalyst composition and calcination temperature upon the physico-chemical properties were closely investigated in relation with the catalytic performances. The result of this investigation indicated the catalysts containing a higher vanadium loading and calcined at 300 °C as the most active. Thus, the VAl07 catalyst led to a selectivity in vitamin K₃ of 54% for a conversion of 2-methylnaphthalene of 76%. Such an activity corresponded to mixtures where metavanadate (Raman line at 940 cm^{–1}) and deca-vanadate (Raman line at 990 cm^{–1}) species were the most abundant. No lines of V₂O₅ (around 705 cm^{–1}) were detected in the catalysts calcined below 600 °C.

© 2015 Elsevier B.V. All rights reserved.

1. Introduction

Quinone derivatives play an important role in bio-systems and are useful intermediates and products of fine chemistry [1]. Besides, aromatic oxidation is one of the key-reactions for the synthesis of vitamin building blocks [2], produced in amounts ranging between 1000 and 10,000 t per year [2]. In this context the development of environmentally benign methods for the production of substituted quinones is still a challenging goal.

Vitamin K₃ (2-methyl-1,4-naphthoquinone, known also as menadione, VK₃) is a synthetic chemical compound sometimes used as a nutritional supplement. It is widely used as a blood coagulating agent due to its anti-hemorrhagic effects and is a key intermediate in the synthesis of the other vitamins of group K. Hence, it is also classified as a provitamin (Scheme 1).

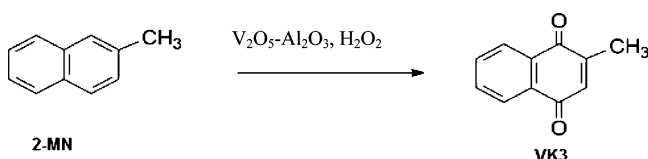
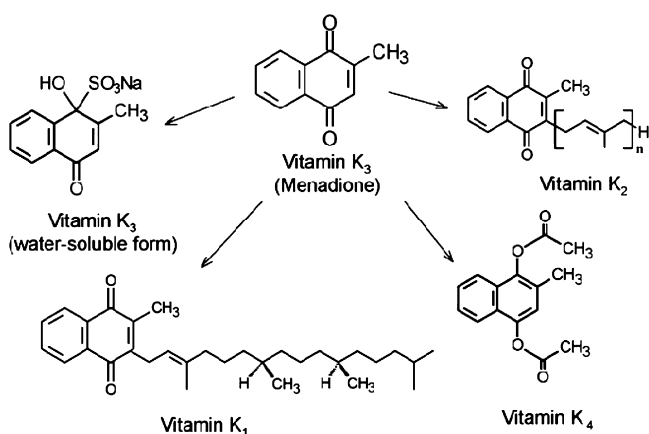
At industrial scale, vitamin K₃ (VK₃) is produced via stoichiometric oxidation of 2-methylnaphthalene (2-MN) by CrO₃ in sulphuric acid and depending on the reaction conditions, the yield to VK₃ is rather poor and does not exceed 40–60% [3]. Moreover, the E-factor (environmental efficiency) is rather unfavorable for the vitamin K₃ production. This method produces about 18 kg of toxic

inorganic waste per 1 kg of target product, and therefore this process is often cited as an example of a "dirty" fine chemical industry process [2]. Also, alternative methods have been proposed to prevent disposal problems of Cr³⁺ and to improve yields and selectivity to VK₃. Both homogeneous and heterogeneous catalysts were considered in this scope [4,5]. CH₃ReO₃ combined with hydrogen peroxide or *tert*-butyl hydroperoxide [6], Pd(II)-modified polystyrenesulfonic acid resins [7], metallophthalocyanine complexes [8] and metalloporphyrin [9] or Ti and Fe containing zeolites [10,11] are among the suggested replacing catalytic systems. In addition to these catalysts, oxidation with Ce methanesulfonate followed by a subsequent electrolytic oxidation of reduced cerium was also suggested [12]. It has also been proposed the use of 2-methyl-1-naphthol as substrate instead of 2-methylnaphthalene [13], but this route involves the catalytic methylation of 1-naphthol, which complicates the technology. Also 2-methyl-1-naphthol is more expensive than 2-methylnaphthalene.

However, the smaller yields and selectivities compared to the initial chromium-based system represent the most important drawbacks of the proposed methodologies. Therefore, designing highly active and selective catalysts for this reaction is still a challenging goal. In this effort, here we report an attempt to selectively oxidize 2-MN to VK₃ using hydrogen peroxide as oxidant agent and vanadia–alumina mixed oxides as catalysts (Scheme 2). Vanadium containing catalysts are still considered among the most promising catalytic systems for oxidation reactions [14], and one of the

* Corresponding author. Tel.: +0040 213675727; fax: +0040 214100241.

E-mail addresses: mihaela.florea@chimie.unibuc.ro, mihaela.florea@g.unibuc.ro (M. Florea), vasile.pavulescu@g.unibuc.ro (V.I. Pârvulescu).



reasons lies in the variability in geometric and electronic structure of surface vanadium oxides in the supported vanadium oxides [15]. In this scope a series of $V_2O_5-Al_2O_3$ were prepared following the co-precipitation method, and calcined at different temperatures. The characterization of these materials was carried out using powder XRD, isotherms of adsorption of nitrogen at $-196^{\circ}C$, Raman spectroscopy, TG-DTA and elemental analysis.

2. Experimental

2.1. Catalyst preparation

Vanadia–alumina mixed oxides with different V/Al ratios were prepared by the co-precipitation of aluminum nitrate (0.08 M) and ammonium metavanadate (0.12 M) solutions at pH 5. Ammonium metavanadate was firstly dissolved in hot water ($60^{\circ}C$) under vigorous stirring, and then acidified with nitric acid (progressively added (drop by drop) until a pH of 3.0). To this solution, the solution containing aluminum nitrate (0.08 M) was added in one charge, and the pH changed to 2.5. Then, the precipitation was achieved with aqueous ammonia (25 wt%) progressively (drop by drop) till a final pH of 5 and the mixture was stirred for another hour. The slurry was subsequently centrifuged and the solid was washed several times with hot water and methanol till the complete removal of nitrates and ammonia ions. Drying was performed in two steps: at $60^{\circ}C$ for 4 h under vacuum, and continued at $120^{\circ}C$, overnight under ambient conditions. Finally, the samples were calcined at 300 or $500^{\circ}C$ for 5 h, in static air. The catalysts were denoted function of the V/Al ratio and calcination temperature (Table 1).

2.2. Physico-chemical characterization

Surface areas were determined by nitrogen adsorption at $-196^{\circ}C$ on a fully computerized Micromeritics ASAP 2020 instrument, using the BET formalism. The catalyst powder was degassed for 2 h at $150^{\circ}C$ and 0.1 Pa before each adsorption measurement.

XRD patterns were recorded with a Shimadzu 7000 powder diffractometer using $Cu K\alpha$ radiation ($\lambda = 1.5418 \text{ \AA}$). The data acquisition was performed in the range $6-80$ 2 theta, with a step of $2^{\circ} \text{ min}^{-1}$.

The chemical composition of the catalysts was determined by inductively coupled plasma (ICP) atomic emission spectroscopy using a Thermo Jarrell Ash Iris Advantage equipment. Prior to analysis the sample was brought into solution by alkali oxidative fusion using $NaOH/Na_2O_2$ and subsequent dissolution with diluted HCl.

Raman spectroscopy was performed using a Horiba spectrometer, equipped with a He-Ne ($\lambda = 633 \text{ nm}$) laser. The spectra were recorded in the $200-1600 \text{ cm}^{-1}$ range.

Thermogravimetry was performed with a Shimadzu DTG-60 instrument under dry nitrogen flow (50 mL min^{-1}), temperature range $25-800^{\circ}C$ with a heating-up rate of $5^{\circ}C \text{ min}^{-1}$. Differential thermal analysis was conducted with a Shimadzu DTA-60 instrument.

Elemental analysis was performed on a EuroEA 3000 automated analyzer. The sample (less than 1 mg) were weighed in tin containers and were burned in a vertical reactor (oxidation tube) in the dynamic mode at $980^{\circ}C$ in an He flow with the addition of O_2 (10 mL) at the instant of sample introduction. Portions of the sample in tin capsules were placed in the automated sampler, from which they were transferred to the oxidation tube at regular intervals. The concentration of each element was calculated using the Callidus program supplied with the analyzer.

2.3. Catalytic tests

The catalytic tests were carried out in a two-necked flask equipped with a magnetic stirrer and a condenser at atmospheric pressure. In a typical procedure, the substrate (2-MN, 2.4 μmole), 0.05 g of catalyst and 5 mL of solvent were loaded into the flask, and then the appropriate hydrogen peroxide (27–30 wt%) was drop wise added ($0.025 \text{ mL min}^{-1}$) using a liquid pump. After H_2O_2 was added totally, the reaction mixture was stirred for different reaction times.

The concentration of hydrogen peroxide prior to use and during the reaction was determined iodometrically. The catalytic experiments were carried out under vigorous stirring at temperatures between 40 and $100^{\circ}C$ and reaction times from 0.5 till 24 h. After completion of 2-MN oxidation and filtering off the catalyst, the mother liquor was diluted 5 times with acetonitrile and the products were analyzed by high-performance liquid chromatography (HPLC) on a Thermo Scientific Accela 600 device equipped with a UV-vis detector and a Mediterranean Sea 18 (C18) column. The mobile phase containing 80% acetonitrile and 20% water was fed at a flow rate of 0.6 mL min^{-1} at $25^{\circ}C$ using a two channels-detection and an injection volume of 3 μL . A maximum of absorption was found for 2-MN at $\lambda = 265 \text{ nm}$ and for VK₃ at $\lambda = 245 \text{ nm}$.

3. Results and discussion

3.1. Catalysts characterization

Table 1 compiles the theoretical and experimental V/Al ratios, BET surface areas, and the nitrogen content determined from the elemental analysis. Surface area varied as function of V/Al ratios and calcination temperatures. As a general trend, the surface area increased with the decrease of the V/Al ratio, with the highest value of $288 \text{ m}^2 \text{ g}^{-1}$ for the VAl01 sample. Fig. 1 shows adsorption isotherms of type IV, with hysteresis loops specific to a capillary condensation characteristic to mesoporous materials. As expected, further calcination at $500^{\circ}C$ induced a further decrease of the surface area, which most probably is associated to a sintering process

Table 1

Surface area of dried and calcined VAI0 catalysts with different V/Al ratios.

Catalyst	V/Al ratio		Surface area ($\text{m}^2 \text{ g}^{-1}$)			N content in dried catalysts (%)
	Theoretical	Experimental	Dried samples	Calcined at (300 °C)	Calcined at (500 °C)	
VAI01	0.1	0.1	288	278	160	2.5
VAI025	0.25	0.25	200	93	71	1.5
VAI05	0.5	0.5	149	117	75	1.2
VAI07	0.7	0.67	140	115	76	1.1
VAI1	1.0	0.93	134	110	70	0.9

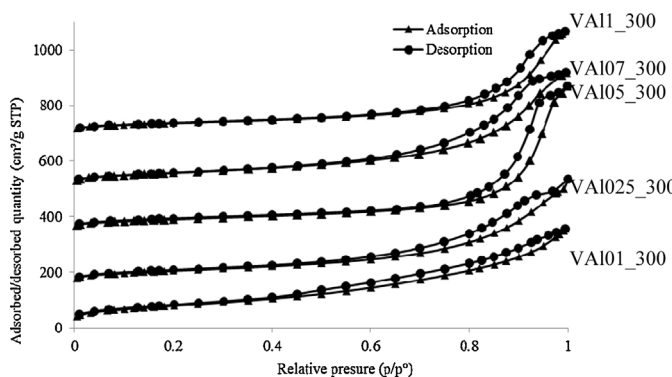


Fig. 1. N_2 adsorption–desorption hysteresis loops for vanadia–alumina mixed oxides catalysts with different V/Al ratios, calcined at 300 °C.

of particles. Data presented in Table 1 indicate that the experimental V/Al molar ratios in the studied catalysts are lower than the theoretical values for the ratios higher than 0.7, most probably due to the poor precipitation of vanadium with aluminum in the starting solution.

Table 1 also presents the nitrogen content in the dried samples. It decreased with the increase of the V/Al ratio and paralleled the decrease of the aluminum nitrate content and the decomposition of ammonium ions in the drying step. After calcination, the nitrogen was completely removed.

Fig. 2 shows the XRD patterns of VAI07 catalyst at different calcination temperatures. As a general tendency, all samples are X-ray amorphous until 500 °C. At 600 °C two well crystallized phases were identified as following: AlVO_4 phase (PDF card 00-039-0276) defined by three diffraction lines at 2 theta = 24.42, 25.68 and

27.68°, and V_2O_5 (PDF card 00-053-0538) defined by diffraction lines at 2 theta = 28.64 and 31.09°. In addition, small reflections lines can be observed at 600 °C (2 theta = 19.4, 37.2 and 45.6°) attributed to $\gamma\text{-Al}_2\text{O}_3$, in agreement with the database standard (PDF card no. 00-010-0425). Similar phases were identified for the other V/Al compositions, as well.

However, the diffractogram of the sample calcined at 900 °C contains less diffraction lines than the one calcined at 600 °C, attributed to only two phases: AlVO_4 and V_2O_5 . Beside this, these patterns shows a dramatic decrease of the intensity of the V_2O_5 characteristic lines while the intensity corresponding to diffraction lines of AlVO_4 increased slowly. Thus, the amount of V_2O_5 which had formed at the lower temperature was most probably depleted due to its reaction with Al_2O_3 followed by the formation of AlVO_4 , especially at higher temperatures.

The DTA curves shown in Fig. 3 revealed for all catalysts two endothermic peaks at 90 and 200 °C, associated with the removal of residual water, nitrate and ammonium ions. An exothermic effect accompanied by a mass loss of around 3% was evidenced for all samples at higher temperatures. For the sample with the lowest V/Al ratio (0.1) it was located at 744 °C and shifted to lower temperatures with the increase of the V/Al ratio. In correlation to the XRD analysis these effects were attributed to the formation of AlVO_4 . For the samples with V/Al ratios of 0.5, 0.7 and 1 an endothermic effect at 759 °C was also evidenced, which can be assigned to the melting of V_2O_5 .

Raman spectroscopy is a useful technique providing informations about the surface vanadium species. According to Weckhuysen and Keller the increase of the vanadium loading may lead to different vanadium oxide species in the following order: orthovanadate (VO_4) → pyrovanadate (V_2O_7) → metavanadate (VO_3)_n → decavanadate ($\text{V}_{10}\text{O}_{28}$) → vanadium pentoxide (V_2O_5) [15]. At low vanadium loadings, isolated four-fold coordinated mono-vanadate species are usually present on the surface. Higher vanadium loadings led to identification of lines in the region 1000–900 cm⁻¹ that are attributed to the V=O stretch vibration of polymeric vanadium species or V_xO_y “clusters” formed on the surface. The Raman lines below 900 cm⁻¹ account to the vibration

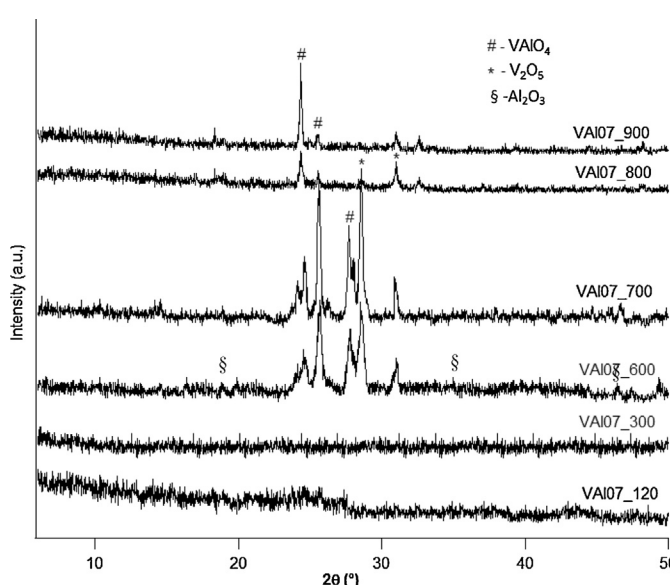


Fig. 2. XRD patterns of VAI07 calcined at different temperatures.

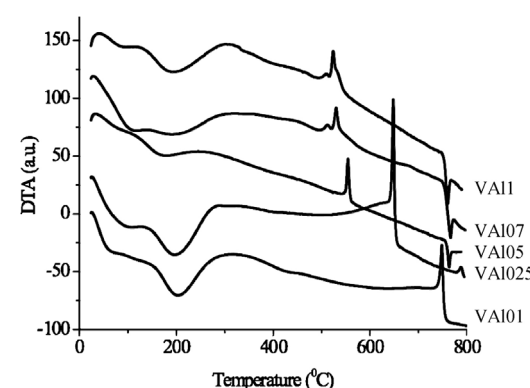


Fig. 3. DTA curves for $\text{V}_2\text{O}_5\text{-Al}_2\text{O}_3$ with different V/Al ratios.

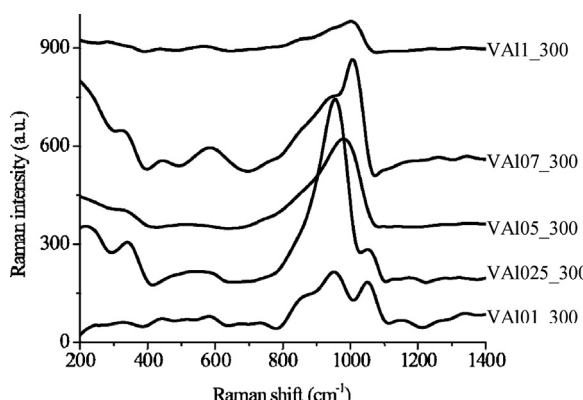


Fig. 4. Raman spectra of VAI0 samples prepared with different V/Al ratios (0.1, 0.25, 0.5, 0.7, and 1) and calcined at 300 °C.

of polymeric V—O—V species [15]. Accordingly, Raman analysis may identify three possible active oxygen sites: terminal V=O, binding surface V—O—V polymeric species, and binding V—O—Al, vanadium to support species. Fig. 4 reveals the Raman spectra of V_2O_5 — Al_2O_3 mixed oxides with different V/Al ratios. The weak and broad Raman lines in the 100–1000 cm⁻¹ region are due to the presence of surface vanadium oxide species on the alumina. Samples VAI01_300 and VAI025_300 show major Raman line at around 950 cm⁻¹, which is accompanied by weak lines at ~560, ~345 and ~220 cm⁻¹. These lines correspond to vanadium in polymeric tetrahedral vanadates and are generated by surface metavanadate (VO_3)_n species [16,17]. Higher V/Al ratios led to a shift of the major line to higher wavenumbers and a new Raman line at 985 cm⁻¹ for VAI05_300 sample and at 1000 cm⁻¹ for VAI07_300 and VAI1_300 samples. This major line is accompanied by a series of broad bands at around 800, 580, 440 and 320 cm⁻¹. According to the literature data [17] we can assume that it accounts for the presence of surface decavanadate $V_{10}O_{28}$ ⁶⁻species [16]. Another argument for the presence of these species can be given with the aid of the Pourboix diagram [18].

The presence of decavanadate species ($H_nV_{10}O_{28}$) is thus justified by the preparation conditions where the precipitation pH was 5. Besides, low vanadium loadings correspond to higher aluminum precursor loadings with a basic character. Accordingly, the basicity of solution increased leading to the formation of vanadium polymeric species, such as (VO_3)_n metavanadates. With the increase of the vanadium loading the acidity of the solutions increased thus leading to the formation of polymeric species such as decavanadates. The presence of V_2O_5 for higher V/Al ratios (0.7 and 1) cannot be excluded, and may be associated to the presence of characteristic Raman lines (287, 310, 490, 540 cm⁻¹).

According to Fig. 4, the samples VAI01_300 and VAI025_300 show a Raman line at 1052 cm⁻¹, which can be assigned most probably to surface residual NO_3^- and is characteristic only for V_2O_5 — Al_2O_3 catalysts with a low vanadium loading. This result is confirmed also by elemental analysis (see Table 1), which point out on the decrease of nitrogen percentage with the increase of the vanadium–aluminum ratio.

The V_2O_5 — Al_2O_3 dried samples also presented lines assigned to surface metavanadate and decavanadate species and their relative concentration depended on the vanadium loading. The influence of the calcination temperature is presented from Raman spectra of the VAI07 sample (Fig. 5). Calcination of the samples at elevated temperatures was accompanied by a decrease of the surface area (Table 1) that corresponded to an increase of the surface vanadium oxide coverage. Different vanadium species were identified as a function of the vanadium loading and calcination temperature. After calcination at 500 or 700 °C the mixture of metavanadate

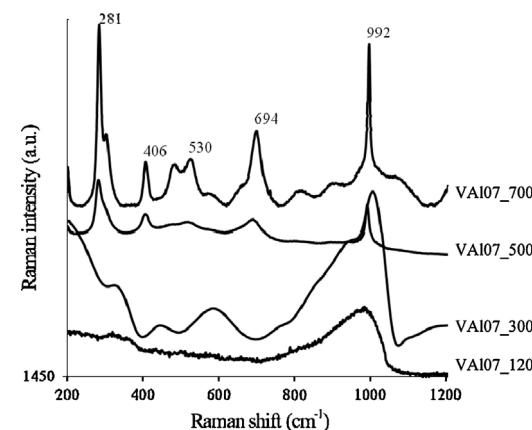


Fig. 5. Raman spectra of VAI07 at different temperatures.

(940 cm⁻¹) and decavanadate (990 cm⁻¹) species observed for VAI07_300, is transformed in decavanadate (992 cm⁻¹) species, as the surface area was reduced from 115 to 76 m² g⁻¹. Calcination at 700 °C, led to sharp Raman lines at 694, 530, 406 and 281 cm⁻¹, which indicates the formation of crystalline V_2O_5 particles.

This result is in agreement with the X-ray diffraction patterns, which presented for the same calcination conditions planes characteristic to V_2O_5 . It is also important to note that the sample calcined at 500 °C (VAI07_500) showed lines characteristics to V_2O_5 nanoparticles, which were not observed in XRD due to the technique limitation (particles <4 nm in size) [19]. The broad line centered at around 900 cm⁻¹ denotes the presence of bridging V—O—Al bonds [20] that are formed by condensation of V—OH and Al—OH during the co-precipitation step.

3.2. Catalytic behavior

Blank experiments in the absence of catalysts indicated no oxidation of 2-MN. The only identified product was acetamide as a result of the reaction of acetonitrile with hydrogen peroxide [21] or by the hydrolysis of acetonitrile under the reaction condition. However, these results infirm the literature reports indicating the formation of VK_3 even in the absence of a catalytic system [10,11]. On the contrary, 2-MN was oxidized to VK_3 on the synthesized catalysts and in order to optimize the reaction the effect of the catalysts structural parameters and reaction conditions was separately investigated.

3.2.1. Effect of the V/Al ratio

The oxidation of 2-MN with H_2O_2 over the catalysts calcined at 300 °C is presented in Fig. 6. The main products were VK_3 and menadiol, but some other complex products, such as those shown in

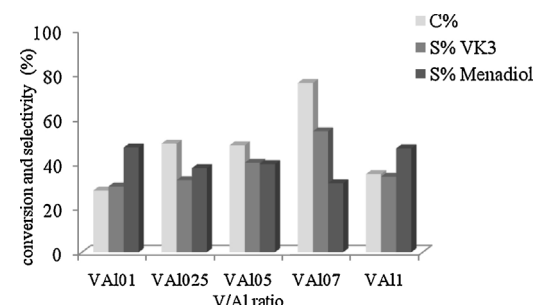
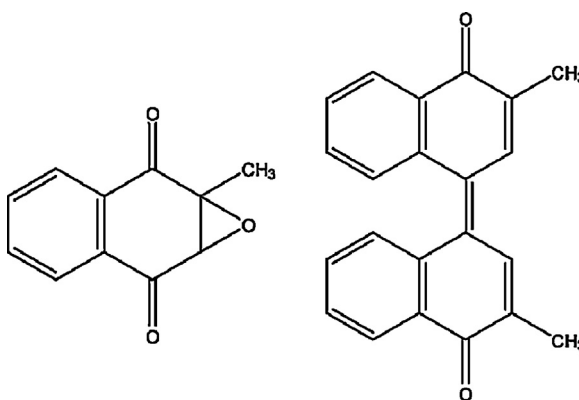


Fig. 6. Conversion of 2-MN and selectivity to VK_3 and menadiol as a function of the V/Al ratio (catalysts calcined at 300 °C, 50 mg catalyst, 2 mL acetonitrile, 80 °C, substrate/ H_2O_2 ratio 1:5, 24 h).



Scheme 3. Other oxidation products identified in 2-MN oxidation.

Scheme 3, were confirmed by GC–MS and H NMR analysis. As a general tendency, the selectivity to VK₃ increased with the vanadium loading, achieving a maximum of 54% for the samples with a V/Al ratio of 0.7. Higher vanadium loadings led to side products such as 2,3-epoxy-2-methyl-1,4-naphthoquinone and 3,3'-dimethyl-[1,1']binaphthylidene-4,4'-dione and as a consequence, the selectivity in VK₃ decreased (32%, for VAI1_300 catalyst). These results, in correlation with the Raman characterization, suggest that the transformation of 2-MN is favored by the presence of decavanadate species. They were well revealed for the VAI07 calcined at 300 °C. However, a further increase in the polymerized vanadate species like for V/Al ratios higher than 0.7 is not favorable for the reaction leading to a decrease of the yields in VK₃. At the end of each reaction, H₂O₂ was almost converted, largely exceeding the amount required by the reaction stoichiometry as a consequence of an over oxidation and of a non-selective decomposition to water and oxygen. The efficiency of H₂O₂ was around 35% for the VAI07 sample and decreased with the decreasing of the V/Al ratio.

3.2.2. Effect of the calcination temperature

According to Fig. 7, within the investigated range of calcination temperatures, 300 °C resulted in the best catalytic activity and selectivity to VK₃ (54%). According to X-ray diffraction this calcination temperature is leading to an amorphous structure, merely constituted from surface metavanadate and decavanadate species (see above Raman results). Higher calcination temperatures where the formation of V₂O₅ started, led to an important increase of selectivity to vitamin K₃, but with the price of a drastic decrease of the conversion (8% for the sample calcined at 700 °C).

Comparative tests with commercial V₂O₅ led also to a very low conversion (5%) and a high selectivity in VK₃. XRD results also proved the formation of V₂O₅ for the samples calcined at 700 °C, thus explaining the low conversion of VAI07_700. A low conversion (4%) was also determined for the catalyst calcined at 500 °C,

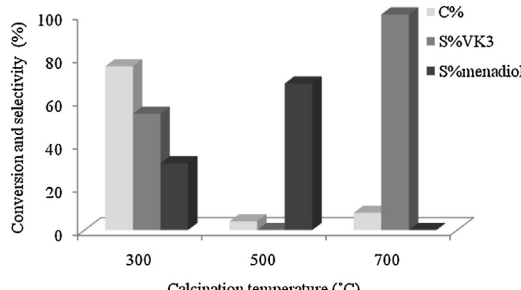


Fig. 7. Influence of the calcination temperature on the catalytic performances (50 mg catalyst VAI07, acetonitrile, substrate/H₂O₂ ratio 1:5, 24 h).

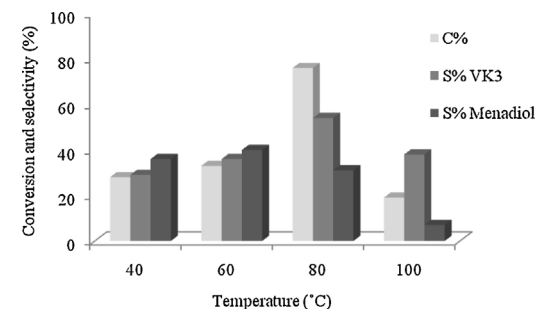


Fig. 8. Influence of temperature on the catalytic performances of the VAI07_300 catalyst (50 mg catalyst, 2 mL acetonitrile, substrate/H₂O₂ ratio 1:5, 24 h).

indicating the fact that the crystallization process already began at this temperature. Indeed, from more sensitive Raman technique it was observed that the spectrum of the sample calcined at 500 °C contains lines characteristics to V₂O₅ that were not evidenced in the X-ray diffraction pattern of this sample.

It results that the highly dispersed metavandate and decavanadate species present in amorphous XRD phase favor the selective oxidation of 2-MN to VK₃. Further decrease of the dispersion increases the selectivity but exhibit a negative effect on the conversion.

3.2.3. Effect of the reaction temperature

Fig. 8 shows the performances of the investigated catalysts in the range of temperature 40–100 °C. After 60 °C, hydrogen peroxide start to be decomposed non-selectively [22]. It appears that the in situ generation of oxygen is benefice for both the conversion and selectivity [23,24]. Higher temperatures than 80 °C generates an additional activation of oxygen leading in the presence of the investigated catalysts to side reactions, i.e. to over-oxidation to 2,3-epoxy-2-methyl-1,4-naphthoquinone or coupling reactions (**Scheme 3**), with a direct effect on the decrease of the selectivity to VK₃. The participation of the radicals leading to side reactions is more probable for temperatures lower than 60 °C [25].

3.2.4. Effect of the substrate/H₂O₂ ratio

Data shown in Fig. 9 indicate that the catalytic performances are influenced by the substrate/H₂O₂ ratio. When the reaction was carried out with a substrate/H₂O₂ ratio of 1:5 a maximum conversion of 76% was measured corresponding to a selectivity in VK₃ of 54%. A higher substrate/H₂O₂ ratio (i.e. 1:3) led to a drastic decrease of the conversion till 17% that was accompanied by a decrease in the selectivity to VK₃. Interestingly enough, when increasing the substrate/H₂O₂ ratio to 1:7 and 1:9, respectively, the conversion remained unchanged (44%), but the selectivity to VK₃ decreased to 26%. Thereby, an excessive content in oxidant leads to a further oxidation of VK₃ to advanced oxidation products issued from

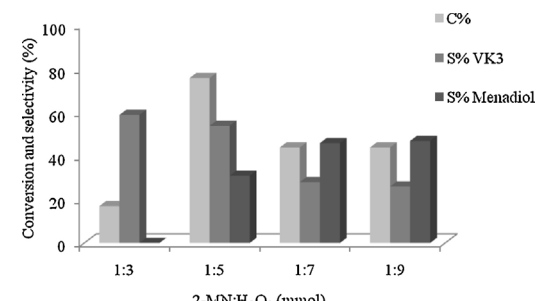


Fig. 9. Influence of substrate/H₂O₂ ratio on the catalytic performances of the VAI07_300 catalyst (50 mg catalyst, 2 mL acetonitrile, 80 °C, 24 h).

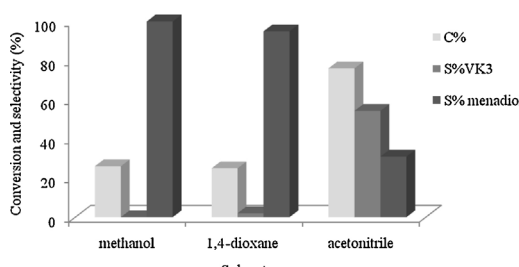


Fig. 10. Influence of the solvent on catalytic performances using the VAI07.300 catalyst (50 mg catalyst, substrate/H₂O₂ ratio 1:5, 80 °C, 24 h).

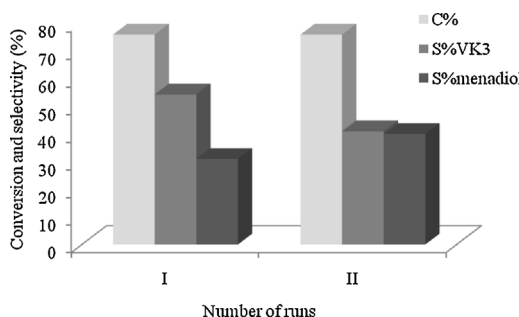


Fig. 11. Leaching tests (run (I) 50 mg of VAI07.300 catalyst, substrate/H₂O₂ ratio 1:5, 2 mL acetonitrile, 80 °C, 24 h; run (II) separated solution from run (I) without catalyst, 80 °C, 24 h).

the methyl group oxidation. On the other side, the formation of larger amounts of water may be a retarding factor since water will participate in a competitive adsorption on the catalysts active centers hindering the formation of vitamin K₃. It appears thus that an optimal substrate/H₂O₂ ratio corresponds to a value of 1:5.

3.2.5. Influence of the solvent

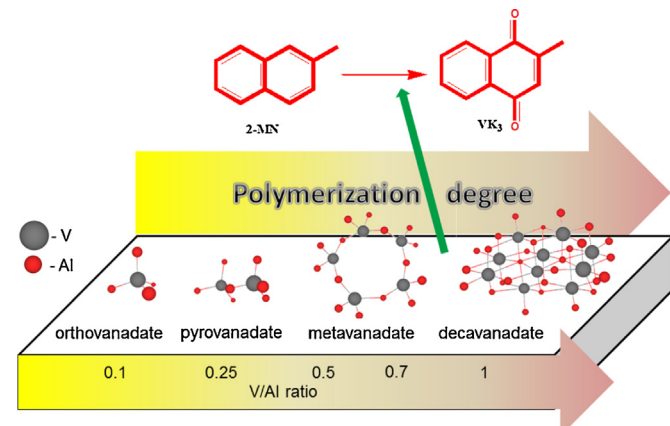
Fig. 10 depicts the influence of various solvents on the catalytic oxidation of 2-MN over the investigated V₂O₅–Al₂O₃ catalysts. While in acetonitrile VAI07 provided a high conversion and selectivity to VK₃, in 1,4-dioxane or methanol the performances were rather poor. It is however difficult to correlate these performances with the physical properties of the investigated solvents. It appears that oxygenated solvent concurs with the substrate to the interaction of the active sites. This process occurs without any additional oxidation of the solvent and only with the oxidation to menadione.

3.2.6. Leaching tests

Leaching of the vanadium species in liquid phase oxidations is a common problem questioning the heterogeneous behavior of the catalysts. In the present experiments leaching was checked by running successive reactions as shown in Fig. 11. In the typical leaching checking procedure the catalyst was separated from the reaction mixture, and the mother liquor was allowed to react further without catalyst (run II). The conversion of the 2-MN and selectivity of vitamin K₃ after run II were 76% and 41%, respectively. According to these results the leaching was insignificant.

4. General assessments

Generally, bulk vanadium oxides are not proper to be used in industrial processes, as they present poor thermal stability and mechanical strength [15]. Therefore in many selective oxidation reactions, vanadium oxide is deposited on oxides such as Al₂O₃, ZrO₂, SiO₂ or TiO₂. The surface structures of supported vanadia on these oxides are quite different to that of bulk. To achieve an



Scheme 4. Type of vanadium entities as a function of the V/Al ratio.

efficient catalyst in this study was considered a preparation procedure in which vanadium and aluminum were co-precipitated.

Scheme 4 shows the evolution of the vanadium entities in the investigated catalysts as a function of the V/Al ratio. This evolution was already verified in oxidation of *o*-xylene to phthalic anhydride on vanadia-based catalysts [26], where the catalytic properties demonstrated that the surface vanadium oxide phase is responsible for the overall catalytic activity and selectivity, while the crystalline V₂O₅ phase exhibits only a minimal effect. This is also in concordance to recent reports of Wachs [14] showing that the surface vanadates are the catalytic active sites for oxidation reactions and that both isolated and polymeric surface vanadia species exhibit the same specific catalytic activity, compared with larger crystalline V₂O₅ nanoparticles that tend to be less active.

Comparing the hydrated and dehydrated (i.e. uncalcined versus calcined) samples, one can observe that the catalytic activity is drastically affected by the thermal treatment. The most active are the samples calcined at 300 °C, as is presented in Fig. 7, where coexists a mixture of metavanadate (Raman line at 940 cm⁻¹) and decavanadate (Raman line at 990 cm⁻¹) species.

5. Conclusions

The results of this study indicate the possibility to enhance both conversion and selectivity in the synthesis of vitamin K₃ through the selective oxidation on heterogeneous catalysts. Particularly for the vanadia–alumina catalysts, the oxidation of 2-MN is favored by the co-existence of deca- and metavanadate species, with an optimal V/Al ratio of 0.7.

Acknowledgements

The authors acknowledge UEFISCDI for the financial support through the project PN-II-TE105/2011.

References

- [1] O.A. Kholdeeva, O.V. Zalomaeva, A.N. Shmakov, M.S. Melgunov, A.B. Sorokin, *J. Catal.* 236 (2005) 62–68.
- [2] W. Bonrath, T. Netscher, *Appl. Catal., A: Gen.* 280 (2005) 55–73.
- [3] R.A. Sheldon, J. Dakka, *Catal. Today* 19 (1994) 215–245.
- [4] S. Biella, G.L. Castiglioni, C. Fumagalli, L. Prati, M. Rossi, *Catal. Today* 72 (2002) 43–49.
- [5] N. Lebrasseur, G.-J. Fan, M. Oxoby, M.A. Looney, S. Quideau, *Tetrahedron* 61 (2005) 1551–1562.
- [6] W.A. Hermann, J.J. Haider, R.W. Fischer, *J. Mol. Catal. A: Chem.* 138 (1999) 115–121.
- [7] S. Yamaguchi, M. Inone, S. Enomoto, *Chem. Lett.* (1985) 827–828.
- [8] C. Pergale, A.B. Sorokin, C.R. Acad. Sci. Paris, Ser. IIc: Chim. 3 (2000) 803–810.
- [9] R. Song, A. Sorokin, J. Bernadou, B. Meunier, *J. Org. Chem.* 62 (1997) 673–678.

- [10] O.A. Anunziata, A.R. Beltramone, J. Cussa, *Appl. Catal., A: Gen.* 270 (2004) 77–85.
- [11] O.A. Anunziata, L.B. Pierella, A.R. Beltramone, *J. Mol. Catal., A: Chem.* 149 (1999) 255–261.
- [12] J. Skarzewski, *Tetrahedron* 40 (1984) 4997–5000.
- [13] K.I. Matveev, V.F. Odyakov, E.G. Zhizhina, *J. Mol. Catal., A: Chem.* 114 (1996) 151–160.
- [14] I.E. Wachs, *Dalton Trans.* 42 (2013) 11762–11769.
- [15] B.M. Weckhuysen, D.E. Keller, *Catal. Today* 78 (2003) 25–46.
- [16] G. Deo, F.D. Hardcastle, M. Richards, I. Wachs, *Am. Chem. Soc., Div. Polym. Chem.* 34 (3) (1989) 529–534.
- [17] G. Deo, I. Wachs, *J. Phys. Chem.* 95 (1991) 5889–5895.
- [18] C.F. BaesJr, R.E. Mesmer, *The Hydrolysis of Cations*, Wiley, New York, NY, 1970.
- [19] I.E. Wachs, C.A. Roberts, *Chem. Soc. Rev.* 39 (2010) 5002–5017.
- [20] N. Magg, B. Immaraporn, J.B. Giorgi, T. Schroeder, M. Baumer, J. Dobler, Z. Wu, E. Kondratenko, M. Cherian, M. Baerns, P.C. Stair, J. Sauer, H.J. Freund, *J. Catal.* 226 (2004) 88–100.
- [21] Y. Ogata, Y. Sawaki, *Tetrahedron* 20 (1964) 2065–20168.
- [22] G. Zi, D. Chen, B. Li, Z. Li, X. Luo, J. Zhang, L. Li, J. Wang, *Catal. Commun.* 49 (2014) 10–14.
- [23] S. Narayanan, K.V.V.S.B.S.R. Murthy, K. Madhusudan Reddy, N. Premchander, *Appl. Catal., A: Gen.* 228 (2002) 161–165.
- [24] D.V. Eremin, L.A. Petrov, *Russ. J. Appl. Chem.* 82 (5) (2009) 866–870.
- [25] G. Strukul, F. Somma, N. Ballarini, F. Cavani, A. Frattini, S. Guidetti, D. Morselli, *Appl. Catal., A: Gen.* 356 (2009) 162–16626.
- [26] B. Grzybowska-Swierkosz, *Appl. Catal., A: Gen.* 157 (1997) 263–310.